Mean field homogenization methods for strand composites

Atul Jain[†]*, *Bo Cheng Jin*, *Steven Nutt*

M.C. Gill Composites Center, University of Southern California
Los Angeles, CA-90016

Published in : Composites Part B: Engineering, Volume 124, 1 Sept. 2017, Pages 31-39
Doi: https://doi.org/10.1016/j.compositesb.2017.05.036.

*corresponding author: atulatj@gmail.com

[†]current affiliation: Department of Mechanical Engineering, Indian Institute of Technology, Kharagpur, India
Email: atuljain@mech.iitkgp.ernet.in

Abstract:

A common method for dealing with in-process manufacturing waste is to cut the prepreg scrap into rectangular strands, and use these strands to produce composites. The properties of the strand composite depend on a number of factors, including the aspect ratio and orientation of the strand. Predictive simulations are required to determine the stiffness of such materials so that optimal composites can be fabricated without extensive experimental testing.

In this work, we present a hybrid method for predicting the stiffness of strand composites by using a combination of finite element and analytic mean field homogenization techniques. The proposed model combines the versatility of finite element models and the ease of computation of analytic schemes. This method can be used to model strands of any shape and orientation distribution; it also presents possibilities for detailed parametric analysis. The proposed method yields predictions that are consistent with experimental measurements and provides insights about testing protocols and observed scatter in experimental results.

1. Introduction

There is increasing use of composite materials in industrial applications, in particularly in the aerospace sector. Increased usage of such materials also leads to increased amounts of waste generated during production. Typically, composites are made by cutting prepreg (short for pre-impregnated fiber) into the desired shape and using a combination of temperature and pressure to achieve compaction. Despite

Please cite this article as "Atul Jain, Bo Cheng Jin, Steven Nutt, **Mean field homogenization methods for strand composites**, Composites Part B: Engineering, Volume 124, 1 September 2017, Pages 31-39, https://doi.org/10.1016/j.compositesb.2017.05.036.

using CAD-based optimization for cutting and shaping, about 20-30% of prepreg tape and fabric is inevitably discarded as scrap. Recently, efforts have been made to fabricate composite laminates out of prepreg scrap by cutting prepreg scrap into rectangular "strands" and using a combination of heat and pressure to achieve compaction [1]. A pictorial representation of the process of converting prepreg scrap to viable composites is presented in **Figure 1**. Thus far, only rectangular strand shapes with random orientation distributions have been considered for this purpose. The stiffness and strength of such materials depends on the shape, aspect ratio, and also the volume fraction of carbon fiber. Feraboli et al. [2,3] showed that the stiffness properties of such materials depend on the strand length.

Figure 1 *In-process prepreg waste; (B) uncured prepreg scrap strands measuring 25 mm by 6 mm; (C) composite hat-stiffened part made from prepreg scrap strands*

Development of optimum composites produced from prepreg scrap requires an understanding of the manufacturing processes as well as the dependence of the properties on the strand shape, orientation, and volume fraction. Due to the large number of possible permutations and combinations, a purely empirical "hit-or-miss" approach is not practical. Additionally, it is not easy to develop test protocols for such non-conventional materials. Modeling of structure-property relations can be helpful to provide a clearer understanding of expected scatter in the experimental quantities. There have been some efforts at understanding the manufacturing of such composites [4,5]. However, models for predicting the stiffness of such materials are limited. Such models can be useful to guide development and to optimize strand composites without the necessity of estensive experimental test campaigns. Here, we present a method for predicting the stiffness of strand composites as a function of shape, orientation, and volume fraction.

In prior work, Selezneva et al. [6,7] proposed an analytic model for predicting the strength of strand composites using a "weakest link" model. This model assumes a two-dimensional strand geometry and orientation distribution. Feraboli et al. [8] used a laminate analogy to develop models for stiffness

Please cite this article as "Atul Jain, Bo Cheng Jin, Steven Nutt, **Mean field homogenization methods for strand composites**, Composites Part B: Engineering, Volume 124, 1 September 2017, Pages 31-39, https://doi.org/10.1016/j.compositesb.2017.05.036.

predictions of strand composites. Such models, however, have major shortcomings. First, they are based on the assumption that the strands have two-dimensional geometries and they retain that geometry after compaction. Secondly, these models are valid only if the orientation distribution of the strand is two-dimensional and uniformly random. Also, only rectangular strands can be modeled by such methods. Often, these assumptions are not valid. Strands can and usually do undergo flexural deformation during manufacturing, and out-of-plane orientation of strand is not uncommmon. Finally, it is desirable to explore alternate shapes in efforts to develop composites with optimum properties.

In the absence of analytic models, one is often tempted to use full finite element (FE) models to calculate the effective stiffness. Such attempts are based on creating a representative volume element (RVE) consisting of composite microstructure and subjecting the RVE to periodic boundary conditions. The applied strain is then related to the average stresses to generate the equivalent stiffness of the material [9]. FE calculations can accommodate any shape of reinforcement, yield accurate results, and also present rich information about local micro-stresses. However, creating representative microstructure models in FE is usually difficult and time consuming. The difficulty in creating the microcstructure increases exponentially as a function of increasing volume fraction of the strand content as it is progressively harder to ensure that the two strands do not intersect each other. Even if one were able to create a representative microstructure, there are additional challenges in meshing and computation. The challenges in meshing are primarily due to the low distance between two adjacent strands, this can either lead to the requirement of a fine mesh or elements which are distorted. The mesh refinement comes at the cost of higher computational cost, and distorted elements lead to erroneous results.

These problems are typically circumvented by making assumptions about the shape and orientation distribution. Jin et al. [9] developed a FE based method for stiffness and damage prediction by idealizing strands as two dimensional plane strain elements, and a similar approach was also used by Picher-Martel et al. [10]. Such assumptions lead to drawbacks similar to those of analytic modeling (limited to two-dimensional uniformly random or aligned distribution of strands).

There are multiple methods based on the solution of Eshelby [11], including, for example, the Mori-Tanaka (MT) formulation [12], self-consistent formulations [13,14], and double interpolative inclusion schemes [15]. Collectively, these are known as the mean field homogenization schemes. Such models

are known to provide reasonable accuracy, and are easy to set up and execute at modest computational cost [16]. However, these models are applicable only for reinforcements which can be approximated as ellipsoids. The reason for the inapplicability of these formulations for non-ellipsoidal inclusions is that there are no analytic solution for Eshelby's tensor [11]. The Eshelby tensor is required to derive the dilute strain concentration, which subsequently leads to the effective stiffness. In contrast, there is no formal restriction to the shape of the inclusion in the mean field assumptions. This is not to say that these schemes have been exclusively used for ellipsoidal inclusions. These schemes have been used to model the effective stiffness of a wide range of materials, either by direct approximation of the inclusion shape to an ellipsoid, or by transforming the inclusion to a family of inclusions. Some examples of applications to composite materials include short fiber reinforced composites [16], short fiber composites with debonded interphase [17], curved fiber composites [18], textile reinforced composites [19], and nanocomposites [20]. Despite the versatility of mean field homogenization schemes, this approach cannot be used to model the stiffness of strand composites. It is not easy to approximate the shape of the prepreg strand to an ellipsoid.

In the context of mean field homogenization schemes, the reinforcement is modeled as an inclusion, and hence the two terms are often used to imply the same thing. Thus, in this work, both reinforcement and inclusion imply a single strand.

Sheet molding compounds (SMC) have internal architecture similar to the composites described in this paper. Attempts have been made to homogenize SMC materials, for example [21]. Also, Jendli et. al. modeled SMC material by treating the fibers as ellipsoids [22].

In this study, mean field homogenization schemes are extended to model the stiffness properties of strand composites by using a combination of finite element calculations and analytic expressions. We propose to create efficient algorithms for generating volume elements (VE) in finite element software which closely replicate the dilute strain condition, and using these algorithms to calculate the Eshelby tensor and implement mean field homogenization schemes. The key advantage of such an approach is that any reinforcement/inclusion shape can be handled, and yet the model is computationally fast and easy to set up, facilitating parametric studies. The accuracy of the proposed model is confirmed using experimental data, and parametric analysis is performed to better understand the scatter in observed properties and to prescribe testing standards for such materials.

Please cite this article as "Atul Jain, Bo Cheng Jin, Steven Nutt, **Mean field homogenization methods for strand composites**, Composites Part B: Engineering, Volume 124, 1 September 2017, Pages 31-39, https://doi.org/10.1016/j.compositesb.2017.05.036.

In general, the mean-field homogenization methods are known to be versatile and capable of being implemented for a wide range of materials. However, it must be acknowledged that compared to full finite element solutions, these methods cannot describe fully the microstress and local stress concentrations. For the purpose of homogenization, the details of stress concentrations are not critical. It has also been reported that the accuracy of these models drop when the concentration of inclusions is high, there are a few methods which are known to be quite accurate for high concentrations [23]. One of the methods developed specifically for this purpose is the double interpolative inclusion [24], which will be used in this paper. Another major criticism of the proposed model is that these models are suspectible to yielding a non-symmetric stiffness tensor which is physically inadmissible [25]. Jain et al. [26] showed that for anisotropic ellipsoid inclusions with a sufficiently large RVE, the degree of non-symmetricity was low. We will recheck this assertion for non-ellipsoid anisotropic inclusions.

In the paper, Section 2 outlines the theory and formulation, Section 3 describes the implementation, and the experiments are recalled in Section 4. The validation of the scheme and analysis is presented in Section 5, and conclusions are given in Section 6.

2. Theory and formulation

In the proposed model, we calculate the stiffness of strand composites using a mean field homogenization scheme. However, instead of the using the analytic expressions of Eshelby for calculation of the Eigen strain and the dilute strain concentration tensors, FE models are built to represent dilute strain concentration conditions. The dilute strain concentration tensor is subsequently extracted and input into the mean field homogenization scheme for the calculation of the stiffness properties. The double interpolative (DI) scheme as proposed by Lielens [24] is chosen as the preferred mean field homogenization scheme, because the volume fraction of carbon fiber in such composites can be as high as ~50%. At high volume fractions, it has been reported previously that the double interpolation scheme is most accurate [23]. In the following two sub-sections, a brief but complete description of the double interpolation scheme and finite element modeling is presented.

2.1 Double interpolative inclusion

In the mean field homogenization, the strain concentration tensor of the inclusions A^{β} is related to the stiffness of the composite using the expression below.

$$C^{eff} = C^m + \sum_{\beta=1}^{M} c_\beta (C^\beta - C^m) A^\beta \quad (1.1)$$

$$\varepsilon_\beta = A^\beta \varepsilon_\infty \quad (1.2)$$

Here, A^β is the strain concentration tensor, C^{eff} is the effective stiffness of the composite, C^m, C^β are the stiffness of the matrix and inclusion respectively, c_β is the volume fraction of the individual inclusion, and M is the total number of inclusions. ε_β and ε_∞ are the strain in the inclusion and the applied far field strain respectively.

The double interpolative inclusion scheme was first proposed by Nemat-Nasser and Hori [15] and later improved by Lielens [24]. This method assumes that the inclusion is embedded in the matrix, which in turn is embedded in a medium in which the stiffness values, C^R, are to be assigned. Two sets of strain concentration factors in the inclusion are calculated by choosing different stiffness values of the medium (C^R), and the strain concentration of the inclusion is obtained by interpolation.

The stiffness of the medium, C^R, is assigned the values of the stiffness of the inclusion, C^β, and the matrix, C^m. Thus, this scheme can be interpreted as an interpolation of the Mori-Tanaka (MT) and inverse MT formulations. The inverse MT formulation corresponds to a MT formulation where the properties of the surrounding medium are the same as those of the inclusion, as opposed to the matrix, during the MT formulation. The former is a good approximation when the volume fraction of the inclusions, v_1, is high, while the latter is a good approximation for low inclusion contents. Thus, an interpolation function which is based on the volume fraction (v_1) was deemed appropriate. The interpolation function, $\zeta(v_1)$ must be a function of the volume fraction and continuous in the region (v_1 = 0, 1). A quadratic function is used in the analysis presented here (eq 2.1).

$$\zeta(v_1) = \frac{1}{2} v_1 (1 + v_1) \quad (2.1)$$

This choice of interpolation function is based on the smoothness and continuity requirements prescribed by Lielens [24], which have been reproduced below

$$\zeta(v_1) > 0,$$
$$\frac{d\zeta}{dv1}(v_1) > 0, \quad (2.2)$$

$$\lim_{v1\to 0}\ \zeta(v_1) = 0,$$

$$\lim_{v1\to 1}\ \zeta(v_1) = 1$$

The strain concentration of the inclusions can thus be calculated using the expression

$$A^{\beta} = \left[\left(1-\zeta(v_1)\right) A_l^{\varepsilon-1} + \zeta(v_1) A_m^{\varepsilon-1}\right]^{-1} \quad (3)$$

where $A_l^{\varepsilon-1}$ and $A_m^{\varepsilon-1}$is the strain concentration factor for the two simulations, viz. Mori-Tanaka (MT) and the inverse MT formulation. Once the strain concentration for each inclusion has been calculated, the effective stiffness of the composite can be calculated using Eqn (1.1). The input for this analysis is the dilute strain concentration tensor, B^m, which relates the strain inside the inclusion subject to the far-field applied strain. The strain concentration tensor for inclusion α, A^{β}, is related to B^m by

$$A^{\beta} = B^{\beta}(c_m I + \textstyle\sum_{\alpha=1}^{M} c_{\alpha} B^{\alpha}) \quad (4.1)$$

$$\varepsilon_{\beta} = A^{\beta}\varepsilon_m \quad (4.2)$$

where, B^{β} is the dilute strain concentration tensor of inclusion β, and c is the volume fraction of inclusions. ε_{β} and ε_m are the strain in the inclusion and the applied far field strain in the matrix respectively when the concentration of the inclusion is dilute.

Here, we propose to calculate the dilute strain concentration tensor using FE methods described in the following sections.

2.2 Calculation of the dilute strain concentration tensor using FE models

The dilute strain concentration tensor relates the strain in an inclusion surrounded by an infinite matrix to the far-field strain. In other words, the dilute strain concentration relates the strain inside the inclusion to the applied strain in the matrix, when the volume concentration of the inclusion is extremely low, such that the inclusion behaves as though it were surrounded by an infinite amount of matrix (see equation 4.2).

The dilute strain concentration can be calculated by finite elements using a model with a large cuboid containing a single inclusion. The centroid of the inclusion and cubic matrix are co-incident. This cubic model is subjected to six uniaxial unit strains, and the average strain in the inclusion is calculated. Each

FE calculation is used to populate a horizontal row of the dilute strain concentration matrix, leading to the 6×6 matrix.

Note that the analysis presented here assumes linear elastic behavior for both the strand and the matrix. However, these methods can be extended to accommodate the non-linear behavior of the composite by accounting for matrix non-linearity [27] and/or damage in the inclusions [17].

3. Implementation

Implementation of the proposed model consists of two major steps. First, the FE volume element consisting of one inclusion is built, and the condition of dilute concentration is confirmed. Next, the double interpolation scheme is implemented. The two steps are described in detail in the following sub-sections.

3.1 FE model building

When the FE model consisting of a single inclusion and matrix is first created, the volume fraction of the inclusion is as low as possible to ensure that the conditions of dilute concentration are met. A cubic matrix with unit dimensions 10 × 10 × 5 is created in FE software (ABAQUS [28]). For the meshing, each of the six cube faces is portioned into three sections. The center part of the cube where the inclusion will be embedded has a fine mesh, and the rest of the cube has a progressively coarser mesh to ensure that the nodes in embedded regions can be tied.

Quadratic tetrahedron elements are used for the meshing, and the strand is meshed using the same quadratic tetrahedron element. The strand is embedded into the matrix volume element such that the centroid of the strand and the matrix are coincident. The use of embedded elements affords benefits during the creation of FE VE. The inclusion and the matrix can be meshed independently, expensive contact algorithms and sectioning of the matrix are not needed, and meshing challenges are minimal [29]. Due to the use of embedded elements, the matrix cube is created and meshed only once, strands with different shapes, aspect ratio etc. can be meshed independently, and an FE model is created. The meshing and the location of the strand are shown in **Figure 2**.

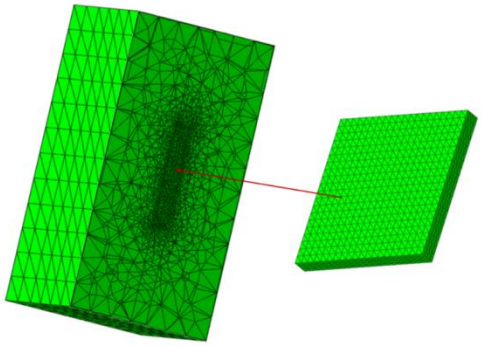

Figure 2 *Meshing of the cube and the inclusion, the matrix cube (in the left) has finer mesh in the regions where the strand will be embedded, while the strand (in the right, zoomed) has uniform fine mesh with sufficient number of elements through the thickness*

A mesh sensitivity analysis of the volume element indicated that there must be at least 6 elements through the thickness of the strand. The mesh size of the core region of the volume element was fractionally smaller than the strand so as to ensure that the embedded equation could be applied by the FE software. The size of the volume element was about one hundred thousand elements for the cubic matrix and less than few thousand elements for the strand. The problem of volume redundancy due to the embedded element technique was resolved using the solution proposed by Tabatabaei and Lomov [30].

Once the volume element has been meshed, it is subjected to periodic boundary conditions and 6 uniaxial strains one by one. The strain concentration tensor is then extracted by volume weighted averaging the strain in each element of the inclusion. The properties of the strand are taken to be that of carbon fiber [31]: E_{11} *= 230 GPa,* E_{22}*=*E_{33}*= 15GPa,* nu_{12} *= 0.2,* nu_{23} *= 0.35 and* G_{12}*= 15 GPa.* Note that in this model, the composite is viewed as a heterogeneous material with carbon fiber interspersed in the matrix. This fundamentally distinguishes this approach from previously developed models. During composite fabrication, the individual existence of the prepreg is somewhat lost, as the matrix of the prepreg mutually inter-fuse and become a single continuum medium in which the fibers are interspersed.

3.2 Check for the dilute strain condition

An important step in the implementation of the proposed scheme is to ensure that the conditions for dilute concentration are met. Theoretically, a concentration is said to be dilute if a single inclusion is included in an "infinite" sea of matrix. However, it is not possible to create a FE volume element with

infinite dimensions. Numerically, the dilute concentration of inclusion is confirmed by creating a volume element with a single inclusion, subjecting it to uniaxial strain, and estimating the resultant average strain in the inclusion. This exercise is repeated for different volume elements with progressively lower volume fractions of the matrix. The concentration of the inclusion is said to be dilute if on further reduction of the volume, there is no change in the average strain in the inclusion.

To confirm dilute strain concentration condition, a series of FE models with matrix (E=3.4GPa, υ = 0.4) and isotropic spherical inclusion (E=100 GPa, υ = 0.2) is created. A spherical isotropic inclusion is chosen so that the average strain FE predictions at dilute concentration can be compared with that of the analytic solution by Eshelby. The volume fraction of the inclusion is progressively reduced, and the average strain in the inclusion is calculated. The average strain in the inclusion as function of the volume fraction is shown in **Figure 3**.

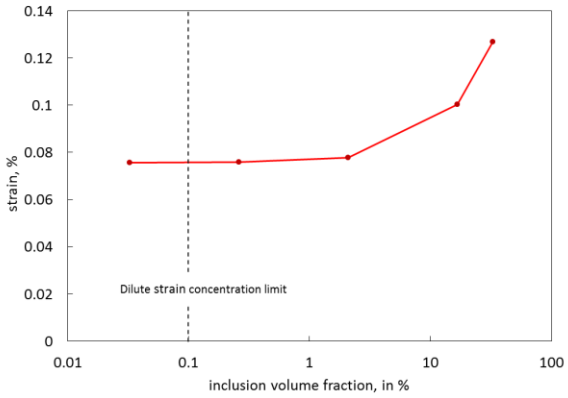

Figure 3 *Average strain in the spherical inclusion. The applied strain in the volume element is 1%, the x-axis is logarithmic*

We are thus confident that a volume fraction of 0.1% or less corresponds to the dilute concentration limit. The dilute strain concentration tensor is calculated using the Eshelby solution and compared with the FE calculation. For an applied load of 1% in the VE, the values of ε_{11}, ε_{12}, ε_{44} derived from the analytic solution were 0.072, 0.009 and 0.12% respectively, and the corresponding values predicted by FE calculations were 0.073, 0.009 and 0.13. Thus, the FE based calculations closely match the analytic solution, confirming once again the dilute concentration limit, as well as use of embedded elements and the volume redundancy correction for small volume fractions. Note that without the volume redundancy correction, the error in the ε_{12} was about 15% with a calculated value of 0.0078%. The ε_{11}, and ε_{44} terms

did not depend strongly on the volume redundancy correction, as the average value in the inclusion with and without the correction was nearly the same. The condition of dilute strain concentration was also checked for flat square inclusions, revealing that the limit of dilute concentration was also ~ 0.1%.

3.3 Implementation of the double interpolation scheme

Once the FE models are built and the dilute strain concentration tensor extracted, the next step is to implement the double interpolation scheme which begins with the creation of the RVE.

The orientation of each strand is represented by a vector ***p*** (say), which in turn is defined by two angles, θ and φ (see figure 4). Mathematically,

$$p_1 = sin\theta cos\varphi$$

$$p_2 = sin\theta sin\varphi \qquad (6)$$

$$p_3 = cos\theta$$

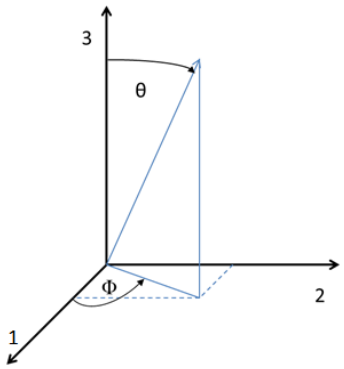

Figure 4 *Illustration of the Euler angles to determine the orientation of the strand*

The angle φ represents the orientation of the strand in the *x-y* plane (in-plane orientation), while the angle θ measured from the *z*-axis represents the out-of-plane orientation. A θ value of -90° implies that the strand has no out-of-plane orientation. For a uniform 2D random distribution of the strand, the value of θ is constant and equal to -90°. Whereas, during the study of out-of-plane orientation, certain ranges of permitted values are prescribed for the angle (90-θ). The angles θ and φ are generated randomly using the "quasi-random number generator" in software (Microsoft Excel) in all the cases presented in this paper to create representative volume elements.

Please cite this article as "Atul Jain, Bo Cheng Jin, Steven Nutt, **Mean field homogenization methods for strand composites**, Composites Part B: Engineering, Volume 124, 1 September 2017, Pages 31-39, https://doi.org/10.1016/j.compositesb.2017.05.036.

Two sets of simulations are performed per AR of strand. In the first set of simulation, the number of strands is approximately the same as the number of strands in the coupons which have been experimentally tested. Based on the dimensions of the coupons (25 × 200× 5 mm) and the measured volume fraction of carbon fiber, we estimate that the approximate number of strands in the 10, 20 and 50 mm strand coupon to be 672, 336 and 135 respectively.

Next, 24 different RVEs with the same number of strands are generated, and the average as well as scatter is evaluated and compared with experimental data. The second set of simulations is performed with a RVE size sufficiently large to remove scatter due to the small number of strands. For this, the number of inclusions is ascertained after a sensitivity analysis, and the number of inclusions in RVE is deemed to be sufficient if the predicted stiffness for different realizations with similar numbers of inclusions is within 5%. (Results of the sensitivity analysis will be presented in Section 5.1). The generation of the RVE and double interpolation scheme is implemented in programming language (C++ in Visual Studio 12.0). A schematic representation of the entire workflow of the scheme is shown in **Figure 5**. In this workflow, the FE based calculations must be performed once, and realization of the RVE and double interpolation scheme can be repeated as often as needed. The FE calculation takes ~ 15 minutes to run on an ordinary desktop PC, while the realization of the RVE and double interpolation scheme takes a fraction of a second.

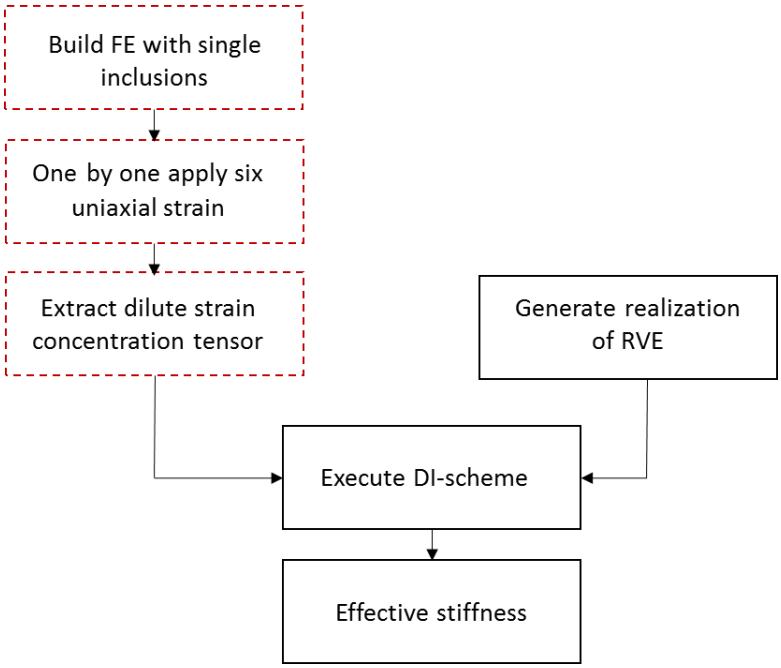

Figure 5 *A flowchart of the proposed algorithm. Items in red dotted boxes are finite element calculations, while the black boxes relate to implementation (in Visual Studio)*

4. Experiments

Rectangular strands were cut from unidirectional prepreg consisting of carbon fiber impregnated with epoxy (CYCOM 5320, Cytec Industries, fiber specification Hexcel IM7 12K [32]). The width of the strands was 10mm, and three lengths were considered: 10, 20 and 50mm. There was some deviation in strand length - the actual maximum and minimum length deviated from the desired length by ~ +/- 5%. The strands were then randomly placed to form a thin layer, and analogous to prepreg (henceforth referred to as "strand prepreg"), these layers were placed one on top of the other. Six layers of strand prepreg was used for fabrication of a single laminate, and each strand prepreg layer weighed ~ 42 grams, leading to a laminate weight of about 250 grams. The laminate dimensions were 216 × 216mm with mean thickness of ~ 3mm (**Figure 6**).

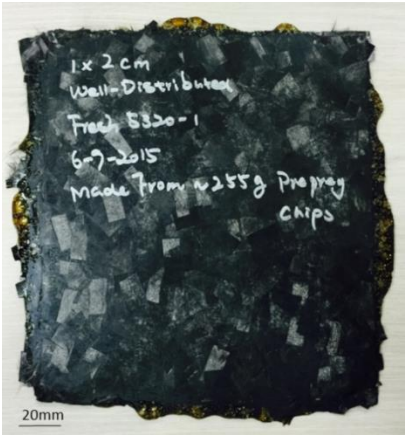

Figure 6 *Laminate made of chopped prepreg with strand dimensions 10mm by 20 mm*

Curing of the panels was achieved by compression molding in a heated platen press (Wabash). The compression force (pressure) of ~ 3.4 MPa was used to reduce the amount of voids and resin bleed on the recommendation of Wei et al. [33]. The curing cycle was 121°C for three hours with a ramp rate of 2.8 °C/minute, followed by a 2-hour free-standing post-cure at 177 °C. The void content in the laminates was measured and derived using X-Ray computer tomography (XCT). XCT settings used were 80 kV and 150 uA, with a 500 ms exposure time, yielding a resolution of 13 μm/pixel. The void content was about 3.3% for the three laminates. The fiber volume fraction was subsequently calculated to be 68% by

weight. A detailed description of the manufacturing methods including comparison of the different methods has been reported [34].

The laminates were then machined to produce coupons for tensile testing, the dimensions of which were 25 × 200mm. Tensile tests were performed according to ASTM standard D3039, the standard for continuous composites. (To the best of our knowledge, there are no ASTM standards for strand composites.) Here, the suitability of this standard for strand composites will be critically examined. End tabs were attached to the coupons, and 5 tensile tests were performed for each strand aspect ratio. The average measured modulus for AR 1, 2 and 5 were 48, 52 and 58 GPa respectively. The ratio of the maximum and minimum measured values for each AR was 1.1, 1.18 and 1.37 respectively. The modulus of the strand composite is comparable to that of aluminum (~60GPa), suggesting that composites fabricated in this fashion could replace aluminum for semi-structural components. However, we acknowledge that comparison of in-plane stiffness is not sufficient to confirm suitability of the material for certain applications, and other relevant properties must also be studied.

Also, the measured modulus increases as the strand size increases. The scatter and variation of the measured modulus was also a function of strand size - coupons with bigger strands showed larger scatter.

5. Results and discussion

In this section, the results of the modeling are presented. First, we present a sensitivity analysis of the modeling, ascertaining the minimum number of strands for creating a representative volume element (RVE) and explaining the scatter observed in the experiments. Next, the predicted values of the model are compared with measured values.

5.1 Sensitivity analysis

Ensuring the "representativeness" of the RVE is the first step towards any homogenization exercise. In the present work, the size of RVE is said to be sufficiently large if the ratio of minimum and maximum predicted stiffness for the same constituent inclusion and matrix but different realizations of the RVE is less than 1.05. A similar sensitivity analysis was performed for fatigue and stiffness properties elsewhere [35]. The number of strands is varied, and 24 different RVE each with same number of strands are created . The ratio of maximum and minimum predicted stiffness for each size of RVE is shown in

Figure 7 for strand aspect ratio 1. The minimum number of strands required for RVE with minimum scatter in simulated properties is 1000.

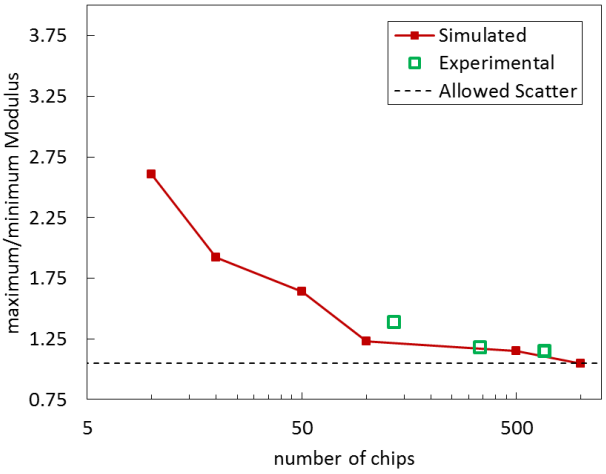

Figure 7 *The scatter in the predicted and measured modulus as a function of the number of strands in the representative volume element (RVE)*

The measured experimental scatter as a function of the number of strands in a coupon is superimposed over the simulated variation in the predicted properties in **Figure 7**, showing that the simulations capture the trend in scatter in observed properties.

Note, also that during the sensitivity analysis, a total of 168 simulations are performed. However, the FE calculations were performed only once, and the rest of the analytic calculations took less than 2 minutes. This represents a significant advantage of this model over conventional finite element modeling, where the finite element models would have to be rebuilt for every simulation, and the computational costs of each simulation would be significantly higher, leading to days of computation, as opposed to few minutes by the proposed method.

5.2 Comparison with experimental values

Comparison of the experimental and predicted values of average stiffness is presented in **Figure 8a,b**. Experimental values match simulated values for coupons having strand aspect ratios 1 and 2 for both the sets of simulation, viz., average of 24 simulations with small RVE and 1 simulation with 1000 strands. In both cases, stiffness is over-predicted slightly for AR 5. The predicted values by averaging 24 simulation are slightly less than the one predicted by the single simulation of 1000 strands.

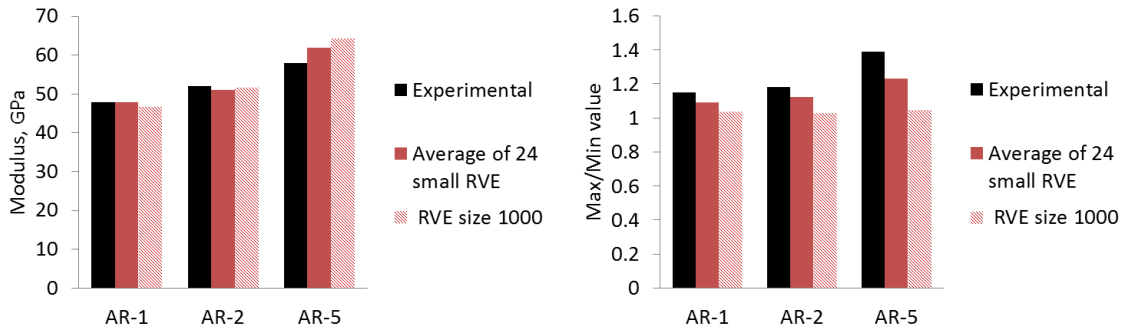

Figure 8 *Comparison of the average experimental modulus and the predicted stiffness (a) comparison of the predicted stiffness, (b) scatter*

The predicted simulation scatter is compared with experimental observations in Figure 8b. As expected, the numerical scatter is a function of the RVE size, and when a smaller RVE with number of strands approximately the same as the experimental coupon is used, we see larger scatter in the simulations. This simulated scatter is similar but less than the observed experimental scatter. When the RVE size is increased to 1000 strands, the numerical scatter almost disappears. From these results, it is clear that the scatter observed during experiments is due to two sources - the first is physical scatter, which is characteristic of the material, and the second is due to insufficient number of strands in the coupons to make it representative of the actual material. We recommend to increase the coupon size such that it includes at least 1000 strands, so that the scatter due to insufficient number of strands can be reduced and the characteristic scatter of the material will be known. Instead of following the ASTM standard, which prescribes a width of 25mm, it is advisable to increase the width as much as the testing equipment permits. Ideally, the width of the coupon must be greater than the width of the largest strand.

5.3 Effect of out of plane orientation and extra matrix

In this sub-section we study the effect of two parameters, *viz*., out-of-plane orientation of the strands and the effect of additional matrix. Both sets of parametric analyses are performed with an RVE size of 1000 strands.

5.3.1 Out of plane orientation

In this sub-section, the effect of out-of-plane orientation distribution of the strand is studied. In the experiments presented, we made special attempts to ensure that all the strands were randomly oriented in the same plane. However, there are manufacturing methods which lead to some out-of-plane orientation

Please cite this article as "Atul Jain, Bo Cheng Jin, Steven Nutt, **Mean field homogenization methods for strand composites**, Composites Part B: Engineering, Volume 124, 1 September 2017, Pages 31-39, https://doi.org/10.1016/j.compositesb.2017.05.036.

of the strand composite [34]. A series of RVE were made with varying ranges of out-of-plane orientation of the strands, and in each case, the maximum out-of-plane angle was prescribed and each strand was prescribed a random out-of-plane orientation value in that range. Note that not all the strands had out-of-plane orientation, but instead the out-of-plane orientation follows a random distribution with the specified range of angles.

The effect of out-of-plane orientation of strand for composites with aspect ratios 1, 2 and 5 is shown in Figure 9a. As expected, the out-of-plane orientation of the strand leads to drop in stiffness and the magnitude of drop increases as the range of out-of-plane orientation increases. The composite with strand AR 5 suffered the greatest loss in stiffness due to out-of-plane orientation of the strand. The predicted loss in stiffness for the AR 1, 2 and 5 was 19.5, 23.4 and 27.9% respectively.

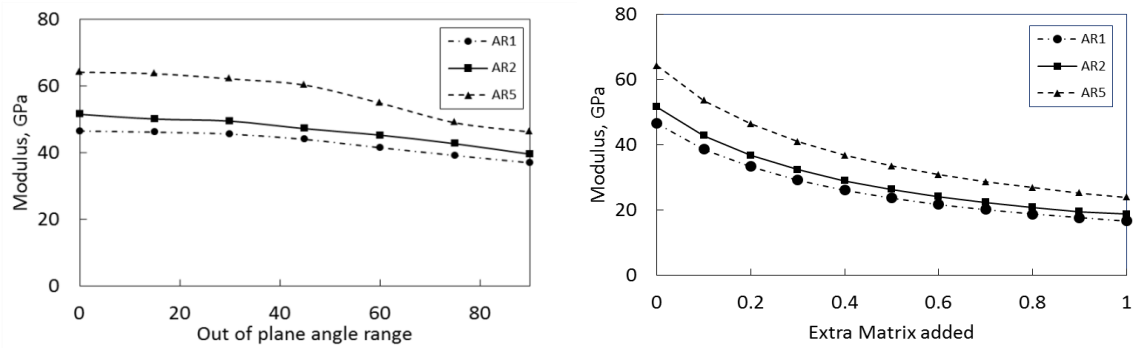

Figure 9 *Parametric studies (a) Effect of out of plane orientation (b) Effect of adding matrix*

5.3.2 Addition of extra matrix

Composites fabricated with cured prepreg can have the tendency to have large numbers of voids. This problem can sometimes be solved by adding extra resin during the manufacturing process. Judicious choice of the grade and quantity of resin can lead to significantly lower voids, better shapability, and increased toughness. In this section, we perform a parametric analysis showing the effect of the extra resin on stiffness. Simulation is performed by introducing extra resin as a fraction of the volume of the prepreg strands. **Figure 9b** shows that the stiffness of composite decreases as we introduce extra resin. The fraction of stiffness drop depended slightly on the aspect ratio of the strand. The stiffness drop if the amount of resin is the same as the initial volume of the strands was 62, 63 and 65% respectively for the three cases (AR =1, 2 and 5) respectively.

Please cite this article as "Atul Jain, Bo Cheng Jin, Steven Nutt, **Mean field homogenization methods for strand composites**, Composites Part B: Engineering, Volume 124, 1 September 2017, Pages 31-39, https://doi.org/10.1016/j.compositesb.2017.05.036.

5.4 A note on the non-symmetric stiffness tensor

A final note concerns the non-symmetric stiffness tensor. A common reservation about the use of mean field homogenization techniques for calculating the effective properties of heterogeneous materials is that the stiffness tensor predicted by the scheme is often non-symmetric, leading to physical inadmissibility conditions [25]. For each of the simulations with 1000 strands, the degree of symmetricity, ΔC_{ij} was determined using the equation

$$\Delta C_{ij} = \frac{C_{ij} - C_{ji}}{C_{ij}}, \text{ i}\neq\text{j} \qquad (6)$$

where C is the stiffness tensor. The maximum degree of asymmetry was on the order of 5-8%. While this is greater than the 0.1% reported by Jain et al. [26] for anisotropic ellipsoid inclusions, this is expected, since the shapes considered here are not regular ellipsoids. However, the degree of asymmetry is not large enough to warrant a full rejection of the proposed scheme. At the end of each simulation, the predicted stiffness is made symmetric by averaging the non-symmetric stiffness and its transpose. This leads to introduction of additional error of ~ 2.5-4 % in the in-plane properties and is not considered critical. One could argue that the use of pseudo-grain discretization techniques [36] or similar variants of the mean field homogenization techniques could be used to avoid a non-symmetric stiffness tensor. However, all known variants of the method guarantee a symmetric stiffness tensor only if the inclusions are isotropic, and the inclusions are anisotropic here. Also, the use of such methods for strands with non-ellipsoid shapes has not yet been explored.

6. Conclusions

A method for calculating the stiffness of strand composites has been developed and demonstrated. The proposed method uses a combination of finite element methods and analytic mean field homogenization methods. The embedded volume technique combined with volume redundancy correction is a viable method to extract the dilute strain concentration tensor, and yields a good match with the analytic solution. A sensitivity analysis shows that at least 1000 strands are required for reliable simulation and testing. Some of the observed experimental scatter is shown to be due to insufficient number of strands, and not due to material property scatter. The simulated results match well with experiment and the degree of asymmetry in the stiffness tensor is limited.

Please cite this article as "Atul Jain, Bo Cheng Jin, Steven Nutt, **Mean field homogenization methods for strand composites**, Composites Part B: Engineering, Volume 124, 1 September 2017, Pages 31-39, https://doi.org/10.1016/j.compositesb.2017.05.036.

The problem of prepreg scrap generated during fabrication of composite parts is rapidly growing. Development of predictive tools like the one proposed in this paper could be an important component of a comphrehensive strategy to guide the design of strand composites made out of prepreg scrap.

Also, in this paper we have developed a homogenization scheme validated for strand composites, this scheme can be easily used to model different types of composite materials with irregular shaped reinforcement for example nano-clay.

7. Acknowledgements

Airbus is thanked for the support of this research through the Airbus Institute for Engineering Research (AIER) at USC. The M.C. Gill Composites Center is also acknowledged for support of this research. Dr. S. A. Tabatabaei is thanked for explaining the use of embedded element technique and the solution to the volume redundancy problem.

8. References

[1] Nilakantan G, Olliges R, Su R, Barnhart J, Nutt SR. Reuse Strategies for Out-of-Autoclave Vacuum-Bag-Only Carbon Fiber-Epoxy Prepreg Scrap. Proc Compos Adv Mater Expo 2014.

[2] Feraboli P, Peitso E, Deleo F, Cleveland T, Stickler PB. Characterization of Prepreg-Based Discontinuous Carbon Fiber/Epoxy Systems. J Reinf Plast Compos 2009;28:1191–214. doi:10.1177/0731684408088883.

[3] Feraboli P, Peitso E, Cleveland T, Stickler PB. Modulus Measurement for Prepreg-based Discontinuous Carbon Fiber/Epoxy Systems. J Compos Mater 2009;43:1947–65. doi:10.1177/0021998309343028.

[4] Levy A, Hubert P. Interstrand void content evolution in compression moulding of randomly oriented strands (ROS) of thermoplastic composites. Compos PART A-APPLIED Sci Manuf 2015;70:121–31. doi:10.1016/j.compositesa.2014.11.017.

[5] Landry B, Hubert P. Experimental study of defect formation during processing of randomly-oriented strand carbon/PEEK composites. Compos PART A-APPLIED Sci Manuf 2015;77:301–9. doi:10.1016/j.compositesa.2015.05.020.

[6] Selezneva M, Roy S, Lessard L, Yousefpour A. Analytical model for prediction of strength and fracture paths characteristic to randomly oriented strand (ROS) composites. Compos Part B Eng 2016;96:103–11. doi:10.1016/j.compositesb.2016.04.017.

[7] Selezneva M, Meldrum S, Roy S, Lessard L, Yousefpour A. Modeling of Mechanical Properties of Randomly Oriented Strand Thermoplastic Composites. Montr QC McGill Univ 2014.

[8] Feraboli P, Cleveland T, Stickler P, Halpin J. Stochastic laminate analogy for simulating the

variability in modulus of discontinuous composite materials. Compos Part A Appl Sci Manuf 2010;41:557–70.

[9] Jin BC, Li X, Jain A, Wu M., Herrarez M., Gonzalez C, et al. Mechanical properties and finite element analysis of reused carbon fiber epoxy composite oriented strand board. Procedings SAMPE 2016, Long Beach, 2016.

[10] Picher-Martel G-P, Levy A, Hubert P. Compression moulding of Carbon/PEEK Randomly-Oriented Strands composites: A 2D Finite Element model to predict the squeeze flow behaviour. Compos Part A Appl Sci Manuf 2016;81:69–77. doi:10.1016/j.compositesa.2015.11.006.

[11] Eshelby JD. The Determination of the Elastic Field of an Ellipsoidal Inclusion, and Related Problems. Proc R Soc London Ser a-Mathematical Phys Sci 1957;241:376–96.

[12] Mori T, Tanaka K. Average Stress in Matrix and Average Elastic Energy of Materials with Misfitting Inclusions. Acta Metall 1973;21:571–4.

[13] Hill R. A self-consistent mechanics of composite materials. J Mech Phys Solids 1965;13:213–22. doi:10.1016/0022-5096(65)90010-4.

[14] Laws N, McLaughlin R. Effect of fiber length on the overall moduli of composite-materials. J Mech Phys Solids 1979;27:1–13. doi:10.1016/0022-5096(79)90007-3.

[15] Nemat-Nasser S., Hori M. Micromechanics: overall properties of heterogeneous materials. 2nd ed. Elsevier; 1999.

[16] Jain A, Lomov S V., Abdin Y, Verpoest I, Van Paepegem W. Pseudo-grain discretization and full Mori Tanaka formulation for random heterogeneous media: Predictive abilities for stresses in individual inclusions and the matrix. Compos Sci Technol 2013;87:86–93. doi:10.1016/j.compscitech.2013.08.009.

[17] Jain A, Abdin Y, Van Paepegem W, Verpoest I, Lomov S V. Effective anisotropic stiffness of inclusions with debonded interface for Eshelby-based models. Compos Struct 2015;131:692–706. doi:10.1016/j.compstruct.2015.06.007.

[18] Abdin Y, Jain A, Verpoest I, Lomov SV. Mean-field based micro-mechanical modelling of short wavy fiber reinforced composites. Compos Part A Appl Sci Manuf 2016. doi:10.1016/j.compositesa.2016.03.022.

[19] Huysmans G, Verpoest I, Van Houtte P. A poly-inclusion approach for the elastic modelling of knitted fabric composites. Acta Mater 1998;46:3003–13. doi:10.1016/s1359-6454(98)00021-4.

[20] Bradshaw R. Fiber waviness in nanotube-reinforced polymer composites—II: modeling via numerical approximation of the dilute strain concentration tensor. Compos Sci Technol 2003;63:1705–22. doi:10.1016/S0266-3538(03)00070-8.

[21] Teodorescu-Draghicescu H, Vlase S. Homogenization and averaging methods to predict elastic properties of pre-impregnated composite materials. Comput Mater Sci 2011;50:1310–4. doi:http://dx.doi.org/10.1016/j.commatsci.2010.04.040.

[22] Jendli Z, Meraghni F, Fitoussi J, Baptiste D. Multi-scales modelling of dynamic behaviour for

Please cite this article as "Atul Jain, Bo Cheng Jin, Steven Nutt, **Mean field homogenization methods for strand composites**, Composites Part B: Engineering, Volume 124, 1 September 2017, Pages 31-39, https://doi.org/10.1016/j.compositesb.2017.05.036.

discontinuous fibre SMC composites. Compos Sci Technol 2009;69:97–103. doi:http://dx.doi.org/10.1016/j.compscitech.2007.10.047.

[23] Klusemann B, Boehm HJ, Svendsen B, Bohm HJ, Svendsen B. Homogenization methods for multi-phase elastic composites with non-elliptical reinforcements: Comparisons and benchmarks. Eur J Mech a-Solids 2011;34:21–37. doi:10.1016/j.euromechsol.2011.12.002.

[24] Lielens G. Micro-Macro Modeling of Structured Materials. Université Catholique de Louvain, Belgium, 1999.

[25] Benveniste Y, Dvorak GJ, Chen T. On Diagonal and Elastic Symmetry of the Approximate Effective Stiffness Tensor of Heterogeneous Media. J Mech Phys Solids 1991;39:927–46.

[26] Jain A, Abdin Y, Van Paepegem W, Verpoest I, Lomov S V. Non-symmetric stiffness tensor prediction by the Mori-Tanaka scheme – Comments on the article "Effective anisotropic stiffness of inclusions with debonded interface for Eshelby-based models, Comp. Structures 131 (2015) 692-706." Compos Struct 2015. doi:10.1016/j.compstruct.2015.08.140.

[27] Pierard O, Gonzalez C, Segurado J, Llorca J, Doghri I. Micromechanics of elasto-plastic materials reinforced with ellipsoidal inclusions. Int J Solids Struct 2007;44:6945–69626962. doi:10.1016/j.ijsolstr.2007.03.019.

[28] ABAQUS. A Gen Finite Elem Software, ABAQUS Inc, Pawtucket RI, USA 2005.

[29] Tabatabaei SA, Lomov S V, Verpoest I. Assessment of embedded element technique in meso-FE modelling of fibre reinforced composites. Compos Struct 2014;107:436–46. doi:http://dx.doi.org/10.1016/j.compstruct.2013.08.020.

[30] Tabatabaei SA, Lomov S V. Eliminating the volume redundancy of embedded elements and yarn interpenetrations in meso-finite element modelling of textile composites. Comput Struct 2015;152:142–54.

[31] Soden PD, Hinton MJ, Kaddour AS. Lamina properties, lay-up configurations and loading conditions for a range of fibre-reinforced composite laminates. Compos Sci Technol 1998;58:1011–22. doi:http://dx.doi.org/10.1016/S0266-3538(98)00078-5.

[32] Cytec n.d. https://www.cytec.com/ (accessed March 20, 2017).

[33] Wu M-S, Centea T, Nutt S, NuttProfessor S, Centea T. Process optimization for compression molding of reused prepreg scrap. Proc. Am. Soc. Compos. - 29th Tech. Conf. ASC 2014; 16th US-Japan Conf. Compos. Mater. ASTM-D30 Meet., 2014.

[34] Jin BC, Li X, Jain A, Gonzalez C, Llorca J, Nutt SR. Optimization of Microstructure and Mechanical Properties of Composite Oriented Strand Board from Reused Prepreg. submitted to Composite Structures, under review

[35] Jain A, Veas JM, Straesser S, Van Paepegem W, Verpoest I, Lomov S V. The Master SN curve approach - A hybrid multi-scale fatigue simulation of short fiber reinforced composites. Compos Part A Appl Sci Manuf 2016:510–8. doi:10.1016/j.compositesa.2015.11.038.

[36] Camacho CW, Tucker CL, Yalvac S, McGee RL. Stiffness and thermal-expansion predictions for

hybrid short fiber composites. Polym Compos 1990;11:229–39. doi:10.1002/pc.750110406.